Available online at www.sciencedirect.com
ScienceDirect
Carbohydrate Research 342 (2007) 1044–1054
Carbohydrate RESEARCH

A Karplus equation for $^3J_{HCCN}$ in amino sugar derivatives

Bruce Coxon*

National Institute of Child Health and Human Development, 31 Center Drive, MSC 2423, National Institutes of Health, Bethesda, MD 20892, USA

Received 5 January 2007; received in revised form 15 February 2007; accepted 20 February 2007
Available online 25 February 2007

Abstract—The ^1H–^{15}N coupling constants of a suite of organic-soluble amino sugar derivatives have been measured by one-dimensional and two-dimensional $^1H/^{15}N$ heteronuclear single quantum, multiple bond correlation (HSQMBC), and the values so obtained are compared with those measured by analysis of ^1H spectra of ^{15}N-labeled amino sugar derivatives. A number of bicyclic amino sugar models have been studied, including methyl 2- (and 3-)amino-4,6-*O*-benzylidene-2- (and 3-)deoxy-α-D-hexopyranosides in chair or skew conformations, and methyl 2,6-anhydro-3-deoxy-3-phthalimido-α-D-mannopyranoside in a locked, almost classical boat conformation. The magnitudes of the vicinal ^1H–^{15}N coupling constants $^3J_{HCCN}$ have been correlated with $^1H/^{15}N$ dihedral angles φ computed for the favored conformations by molecular dynamics with molecular mechanics energy minimization. Nonlinear regression of the coupling constants on the dihedral angles has yielded a Karplus equation: $^3J_{HCCN} = 3.1\cos^2\varphi - 0.6\cos\varphi + 0.4$.

The coefficients of the terms in this equation have been compared with those reported for 15 other pairs of nuclei, and the coefficient of the important $\cos^2\varphi$ term found to be numerically smallest for $^3J_{HCCN}$.
Published by Elsevier Ltd.

Keywords: Amino sugars; ^{13}C NMR chemical shifts; COSY; Cryoprobe; ^1H NMR chemical shifts; HMBC; HSQC; HSQMBC; Karplus equation; Molecular dynamics; ^{15}N NMR coupling constants

1. Introduction

Amino sugar derivatives are widespread in nature, forming important structural elements of aminoglycoside antibiotics, blood-group substances, exoskeletal materials, and bacterial polysaccharides used in vaccine development.[1] We are interested in extending the use of ^{15}N NMR parameters for the structural, stereochemical, and conformational analysis of biological materials, in this instance, by definition of the dependence of vicinal ^1H–^{15}N coupling constants ($^3J_{HCCN}$) on the $^1H/^{15}N$ atomic dihedral angle in amino sugars. The dependence of vicinal ^1H–^1H coupling constants on the dihedral angle[2,3] and on a number of other molecular parameters is now well established for carbohydrates[4–6] and other molecules.[7–12] Considerable data exist also for the dependence of three-bond ^1H–^{13}C coupling constants, for both the HCOC[13–21] and HCCC[14,22–24] moieties. However, the dependence of $^3J_{HCCN}$ on dihedral angle and on other molecular parameters is less well defined,[25] especially in amino sugars. Our approach has been to measure the $^3J_{HCCN}$ values of amino sugar derivatives in fixed or known conformations, in which the ^1H and ^{15}N nuclei have defined orientations. Many of our model compounds are methyl 2- (and 3-)amino-4,6-*O*-benzylidene-2- (and 3-)deoxy-α-D-hexopyranosides, which are known for their conformational purity in chair conformations,[26] or occasionally a skew form.[27–29] Like *trans*-decalin, trans fusion of the 4,6-*O*-benzylidene ring to the pyranose ring restricts the number of conformational possibilities, so that the latter ring cannot adopt an alternative chair form.

Also studied, was methyl 2,6-anhydro-3-deoxy-3-phthalimido-α-D-mannopyranoside, which exists in a locked, almost classical boat conformation.[30] $^1H/^{15}N$ dihedral angles in the amino sugar models have been

* Tel.: +1 301 2954780; fax: +1 301 2951435; e-mail: coxonb@mail.nih.gov

0008-6215/$ - see front matter Published by Elsevier Ltd.
doi:10.1016/j.carres.2007.02.023

defined by molecular dynamics computations, followed by energy minimization by molecular mechanics.

2. Experimental

2.1. Materials

Methyl 2-amino-4,6-*O*-benzylidene-2-deoxy-α-D-altropyranoside[31] (**1**), methyl 4,6-*O*-benzylidene-2-deoxy-2-phthalimido-α-D-altropyranoside[31] (**2**), methyl *N*-2′,4′-dinitrophenyl-3-amino-4,6-*O*-benzylidene-3-deoxy-α-D-altropyranoside[26] (**3**), methyl *N*-2′,4′-dinitrophenyl-3-amino-4,6-*O*-benzylidene-3-deoxy-2-*O*-methyl-α-D-altropyranoside[26] (**4**), methyl 2-*O*-acetyl-*N*-2′,4′-dinitrophenyl-3-amino-4,6-*O*-benzylidene-3-deoxy-α-D-altropyranoside[26] (**5**), bis(methyl 2-*O*-acetyl-4,6-*O*-benzylidene-3-deoxy-α-D-altropyranosid-3-yl)amine[32] (**6**), methyl 3-amino-4,6-*O*-benzylidene-3-deoxy-α-D-glucopyranoside[31] (**7**), methyl 4,6-*O*-benzylidene-3-deoxy-3-phthalimido-α-D-altropyranoside[29] (**8**), methyl 2,6-anhydro-3-deoxy-3-phthalimido-α-D-mannopyranoside[30] (**9**) (see Fig. 1). Compounds **2**, **8**, and **9** were also available in ^{15}N-labeled form.

2.2. NMR spectroscopy

NMR spectra were acquired at 300 K by use of a Bruker DRX-500 NMR spectrometer equipped with a 5 mm TXI HCN cryoprobe with *z*-gradient coil, and a Silicon Graphics (SGI) O2 workstation, changing to an HP xw4200 PC workstation. Bruker XWINNMR software, version 3.5.6 running under IRIX 6.5.27 was used for the SGI system, and TopSpin 1.3.4 running under Windows XP Pro SP2 for the HP workstation. ^{1}H NMR spectra were acquired using a spectral width of 5.48 kHz, and 32,768 point data sets, zero-filled or linear predicted to 65,536 points, a 30° pulse (2.4 μs), and a pulse recycle time of 6 s. NMR solvent volumes were 0.5 mL of $CDCl_3$ unless stated otherwise, and solute weights were ~1 mg (5–9 mM) for ^{15}N-labeled compounds, and 20–30 mg (90–215 mM) for unlabeled derivatives. Tetramethylsilane was used as an internal chemical shift reference ($\delta = 0$) for ^{1}H and ^{13}C NMR spectra. The resolution of the spectra was enhanced by Gaussian multiplication of the free induction decay, using a line-narrowing of −0.5 to −6.0 Hz, and a Gaussian truncation fraction of 0.3. Assignments of ^{1}H–^{1}H coupling constants, including long-range couplings, were confirmed by digital homodecoupling. In order to obtain sharp ^{1}H spin–spin multiplets suitable for measurement of coupling constants, it was important that the OH and NH protons not be in an intermediate rate of exchange, since this led to broadening of the signals of nearby CH protons. Occasionally, traces of acid were removed from $CDCl_3$ solutions by the addition of up to four beads of molecular sieves to the NMR sample tube, without affecting field homogeneity significantly. Fully coupled hydroxyl proton spectra were obtained in this way. However, such spectra were more reliably acquired by use of acetone-d_6 as solvent. On the other hand, in $CDCl_3$ solution, the presence of a free amino group in

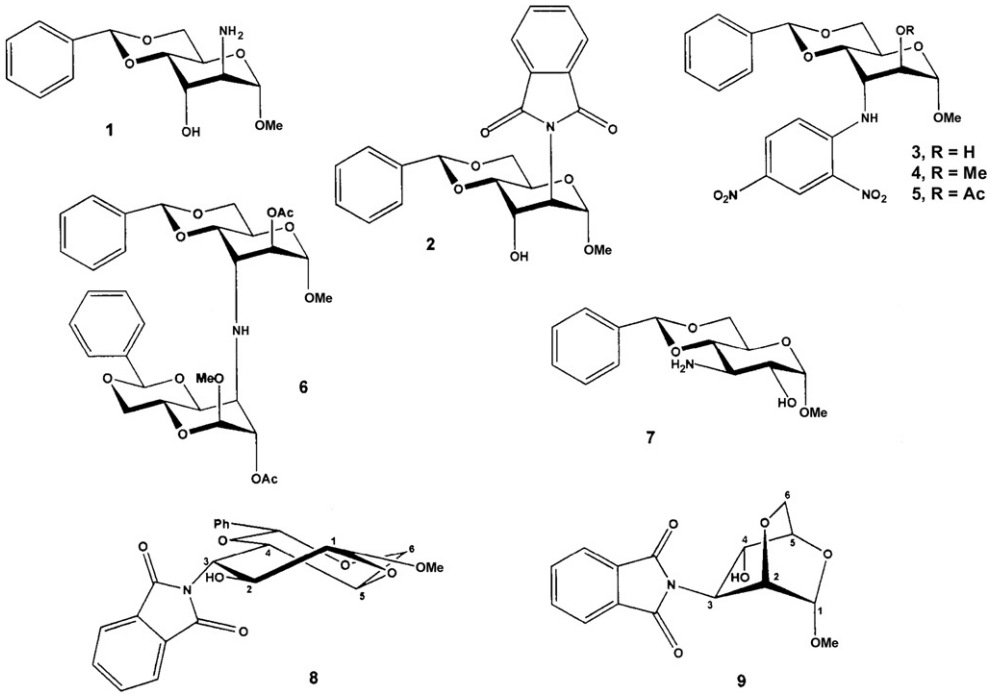

Figure 1. Target compounds (**1**–**9**) for measurement of ^{1}H–^{15}N coupling constants.

derivatives **1** and **7** catalyzed an increased rate of proton exchange of NH_2 and OH groups, thus giving decoupled multiplets that were also good for the purpose.

^{13}C NMR spectra were acquired by using 65,536 point data sets, a 45° pulse (6.7 μs), and a pulse recycle time of 2 s. Resolution was enhanced either by zero-filling to 65,536 data points, or by forward, complex linear prediction to 131,072 points, together with Gaussian multiplication by way of a line-narrowing of −0.5 to −4 Hz, and a Gaussian truncation fraction of 0.3. Values of $^1J_{C\text{-}1,H\text{-}1}$ were measured either from ^1H-coupled, 1D ^{13}C NMR spectra acquired with the nuclear Overhauser effect (NOE) by use of gated, WALTZ-16 irradiation at the ^1H frequency, or from ^1H-coupled 2D HSQC spectra obtained from 4096 (t_2) × 512 (t_1) point data sets, zero-filled to 8192 (F_2) × 2048 (F_1) points.

All 2D NMR spectra were acquired by pulsed field gradient-selected methods. 2D correlation spectroscopy (COSY) and homodecoupling were used to confirm ^1H assignments, and heteronuclear single quantum correlation (HSQC) and heteronuclear multiple bond correlation (HMBC) were used for ^{13}C assignments. 2D COSY and HMBC NMR spectra were obtained by using 2048 (t_2) × 512 (t_1) point data sets, zero-filled to 2048 (F_2) × 2048 (F_1) points, whereas 2D HSQC spectra were taken from 2048 (t_2) × 512 (t_1) point data sets, linearly predicted to 4096 (F_2) × 4096 (F_1) points. For 2D COSY, the read pulse was 30° (2.4 μs). 2D HSQC and HMBC were acquired with ^1H and ^{13}C spectral widths of 5.48 kHz (F_2) and 25.1 kHz (F_1), respectively.

1D and 2D $^1H/^{15}N$ heteronuclear single quantum, multiple bond correlation (HSQMBC) NMR spectra[33,34] were acquired by using a Bruker *hsqcetf3gpjclrnd* pulse sequence, which included shaped, 180° chirp pulses of 500 μs and 2 ms for inversion and refocusing, respectively, at the ^{15}N frequency. A pulse sequence execution error in the form of non-progressive accumulation of data was eliminated by setting separate, but equal phase programs (ph14 = 0 0 0 0 0 2 2 2 2 and ph4 = 0 0 0 0 0 2 2 2 2) for the shaped ^{15}N refocusing pulse and the following ^{15}N 90° high power pulse, respectively. The 1/2J delay was calculated from $^1J_{NH}$ 93 Hz, whereas the evolution delay for long-range ^1H–^{15}N coupling constants was 83 ms. 1D HSQMBC was conducted by using 16,384 point data sets, linearly predicted to 65,536 points.

For 2D HSQMBC, data sets of 16,384 (t_2) × 256 (t_1) points were used, which were linearly predicted to 32,768 ($F_2 = {}^1H$) × 1024 ($F_1 = {}^{15}N$) points, with spectral widths of 5.48 kHz and 10.14 kHz, respectively. Display of the HSQMBC spectra was optimized by testing various window functions ranging from exponential filtering with a line-broadening of 0.2 Hz to Gaussian multiplication with line-narrowing of up to −2 Hz. 2D COSY and HMBC spectra were displayed in the magnitude mode, whereas the phase-sensitive, echo–anti-echo protocol was used for ^1H-coupled 2D HSQC, ^{13}C decoupled 2D HSQC, and 2D $^1H/^{15}N$ HSQMBC. The anti-phase spectra obtained by the HSQMBC technique were analyzed by the 'multiplet total width subtraction' method based on the fact that for first-order multiplets, the total width of the multiplet, that is, the distance in hertz between its outer maxima, is equal to the sum of the coupling constants in the multiplet. Therefore, the additional J_{HCCN} coupling constant that appears in the ^1H–^{15}N HSQMBC multiplet may be calculated by subtracting the total width of the corresponding multiplet in a reference 1D ^1H NMR spectrum acquired under the same conditions from the total width of the HSQMBC multiplet.

2.3. Molecular modeling

Molecular modeling computations were performed with a Silicon Graphics, Inc. Octane workstation, equipped with an R-10000 250 MHz CPU and Accelrys Insight II/Discover software, version 2000.1. For each amino sugar derivative, the conformational type was identified from the values of the three-bond, four-bond, and five-bond coupling constants (Table 3), and this conformation was built in the Biopolymer module of the Insight II/Discover software. The initial models of compounds **3**–**5** were built with planar *N*-2′,4′-dinitrophenylamino groups. At 300 K, each conformation was subjected to an initial steepest descent energy minimization for 5000 steps, until the r.m.s. derivative was <0.001. An AMBER forcefield was used that included Homans' parameters[35] for the anomeric atoms. The computations were performed with implicit solvent, by use of a distance dependent, effective dielectric constant of 4.0. At 300 K, 1000 equilibration steps of 1 fs each were run, followed by 5000 molecular dynamics steps of 1 fs each, and then VA09A energy minimization. The molecular dynamics and mechanics calculations were then repeated five times, until constancy of dihedral angles could be seen. Dihedral angles of interest were then measured from the energy-minimized model, using the Insight II/Discover program. For compounds **8** and **9**, the required geometries were obtained from data for previous publications.[29,30]

3. Results and discussion

3.1. Multinuclear NMR data and molecular dynamics

Measurement of the coupling constants was performed by 1D ^1H NMR of ^{15}N-labeled amino sugars[30,31,36–38] and/or 1D and 2D $^1H/^{15}N$ HSQMBC[33,34] of amino sugars having ^{15}N either enriched or at natural abundance. The latter experiments were facilitated by the enhanced sensitivity of a $^1H/^{13}C/^{15}N$ inverse NMR cryoprobe which yielded excellent HSQMBC spectra from 1 mg

of ^{15}N-labeled derivative, or from 20 to 30 mg having ^{15}N at natural abundance. Several of the compounds **1**–**9** have been studied before,[26,29–32] but generally at lower magnetic field strengths. Re-examination of these compounds using a modern NMR spectrometer has resulted in complete ^{1}H and ^{13}C chemical shift and coupling constant assignments and more precise chemical shifts and coupling constants than heretofore, and the application of vigorous resolution enhancement methods has led to the discovery of a number of small long-range coupling constants that were not detected previously. Full spectral analyses have not been presented previously for compounds **3**–**5** and **8**-^{15}N.

^{1}H chemical shifts of derivatives **1**–**9** are reported in Table 1, their ^{13}C chemical shifts in Table 2, and ^{1}H–^{1}H coupling constants and $^{1}J_{C\text{-}1,H\text{-}1}$ values in Table 3. The latter values in the range 167.2–173.1 Hz served to confirm the α anomeric configuration of all the derivatives. The ^{1}H chemical shifts of the phenyl protons in **1**–**8** were obtained from listings of 2D ^{1}H/^{13}C HSQC cross peaks, instead of by direct analysis of the complex ^{1}H NMR spectra.

For compounds **1**–**6**, the ranges of values $J_{1,2}$ 1.1–1.7, $J_{2,3}$ 2.3–3.1, $J_{3,4}$ 3.0–3.8, and $J_{4,5}$ 9.6–9.9 Hz (Table 3) indicate that the pyranose ring of all of these derivatives adopts the $^{4}C_{1}$ form, as depicted in Figure 1. Also consistent with this form is the W-type, long-range coupling $^{4}J_{1,3}$ 0.6–1.1 Hz observed for **1**–**6** (Table 3). A number of small, non-W long-range couplings were also measured for **1**–**6**: $^{4}J_{1,5}$ 0.5–0.7, $^{4}J_{2,4}$ 0.4, and $^{4}J_{3,5}$ 0.6 Hz. An extended W-type, long-range coupling $^{5}J_{3,6}$ 0.5–0.7 Hz was also detected for **1**–**6**, a coupling constant that appears to be characteristic of the in-plane arrangement of H-3, C-3, C-4, C-5, C-6, and H-6e in the $^{4}C_{1}$ form, when measured under high resolution. In derivatives **7** and **8**, H-3 is out of the plane defined by C-3, C-4, C-5, C-6, and H-6e, and $^{5}J_{3,6}$ was not detected. Neither was it detectable for the 2,6-anhydro-mannoside **9**, in which H-3 is axial. As demonstrated previously from the vicinal ^{1}H–^{1}H coupling constants, the pyranose rings of compounds **8** and **9** adopt the $^{1}S_{5}$ skew boat form[29] and slightly twisted $^{O}B^{6}$ boat form,[30] respectively.

^{1}H–^{15}N and ^{13}C–^{15}N coupling constants for compounds **1**, **2**-^{15}N, **6**, **7**, **8**-^{15}N, and **9**-^{15}N are reported in Table 4, together with dihedral angles for certain ^{1}H/^{15}N pairs, as computed by molecular dynamics. These dihedral angles are comprised of two types: (a) single values that correspond to couplings over three bonds, and (b) dual values that represent the angles subtended by four bonds.[39] Compounds **8** and **9** provide unusual dihedral angles over three bonds, $\varphi_{4,N\text{-}3}$ 142° and 10°, respectively. The latter angle represents the slight degree of twist of the boat conformation of **9** away from the eclipsed orientation of N-3 and H-4 (compare the undistorted boat form of **9** shown in Fig. 2 with the

Table 1. ^{1}H chemical shifts (ppm) of amino sugar derivatives

Derivative	R-2	R-3	H-1	H-2	H-3	H-4	H-5	H-6	H-6′	OMe	PhC*H*	Ph H-2,6	H-3,5	H-4	PHTH H-2,5	H-3,4	DNP H-3	H-5	H-6	Others
1	NH_2	OH	4.553	3.290	3.960	3.891	4.213	4.331	3.809	3.419	5.624	7.501	7.362	7.358	—	—	—	—	—	—
2	PHTHN[a]	OH	4.838	4.731	4.312	4.605	4.356	4.434	3.932	3.431	5.744	7.498	7.394	7.385	7.883	7.767	—	—	—	HO-3 2.704
3	OH	DNPNH[b]	4.783	4.141	4.429	4.353	4.134	4.330	3.888	3.585	5.617	7.185	7.236	7.281	—	—	9.113	8.118	7.214	HO-2 2.459
4	OMe	DNPNH	4.880	3.638	4.473	4.267	4.104	4.313	3.872	3.590	5.596	7.190[c]	7.240[c]	7.285[c]	—	—	9.115	8.126	7.246[c]	OMe-2 3.554
5	OAc	DNPNH	4.798	5.099	4.421	4.231	4.180	4.353	3.893	3.576	5.628	7.201	7.229	7.279	—	—	9.121	8.139	7.211	OAc 2.226
6[d]	OAc	Alt*p*NH[e]	4.599	5.026	3.326	3.846	4.174	4.238	3.767	3.416	5.624	7.470	7.337	7.329	—	—	—	—	—	OAc 1.989
7	OH	NH_2	4.710	3.574	3.202	3.353	3.770	4.256	3.701	3.424	5.502	7.475	7.356	7.351	—	—	—	—	—	HO-2 3.153
																				H_2N-3 3.153
8-^{15}N	OH	PHTHN	4.685	4.954	4.804	4.053	4.672	4.400	3.662	3.511	5.458	7.209	7.159	7.206	7.843	7.704	—	—	—	HO-2 2.322
9	OH (R-4)	PHTHN	5.094	3.784	4.763	4.912	4.146	4.400	4.050	3.574	—	—	—	—	7.837	7.727	—	—	—	HO-4 3.469

[a] Phthalimido.
[b] *N*-2′,4′-Dinitrophenylamino.
[c] From Ref. 56.
[d] In acetone-d_6.
[e] Methyl 2-*O*-acetyl-4,6-*O*-benzylidene-3-deoxy-α-**D**-altropyranosid-3-yl-amino.

Table 2. ^{13}C chemical shifts (ppm) of amino sugar derivatives

Derivative	R-2	R-3	C-1	C-2	C-3	C-4	C-5	C-6	OMe	Ph*C*H	Ph C-1	C-2,6	C-3,5	C-4	C-1,6[a]	C-2,5[a]	C-3,4[a]	C=O	DNP C-1,2,3 C-4,5,6
1	NH_2	OH	103.29	54.38	70.67	76.40	58.51	69.24	55.68	102.31	137.28	126.25	128.30	129.17	—	—	—	—	
2-^{15}**N**	PHTHN[a]	OH	99.71d[b]	55.21d	67.79d	76.10	57.95	69.49	55.59	102.04	137.19	126.24	128.38	129.30	131.49d	123.58d	134.46	167.69d	—
3	OH	DNPNH[c]	100.74	69.69	53.50	76.27	59.44	68.98	55.35	102.03	136.67	125.73	128.22	129.22	—	—	—	—	148.88 130.75 124.03 136.07 129.18 115.76
4[*]	OMe	DNPNH	98.20	78.58	51.13	76.54	59.23	68.96	55.23	101.94	136.76	125.74	128.19	129.17	—	—	—	—	148.84 130.80 123.96 136.14 129.14 115.78
5	OAc	DNPNH	98.32	70.08	51.09	76.22	59.11	68.89	55.47	102.08	136.56	125.76	128.23	129.26	—	—	—	169.42	148.56 130.98 123.93 136.38 129.30 115.62
6	OAc	Alt*p*NH[d]	99.68	73.50	56.66	78.73	59.18	69.59	55.39	102.66	139.39	127.35	128.78	129.44	—	—	—	169.78	—
7	OH	NH_2	99.58	72.31	53.39	81.08	62.73	69.00	55.45	101.77	137.19	126.23	128.32	129.19	—	—	—	—	—
8-^{15}**N**	OH	PHTHN	101.92d	67.81	50.72d	73.99d	63.48	70.07	55.96	101.76	137.10	126.15	128.06	128.94	131.81d	123.32d	134.00	168.61d	—
9-^{15}**N**	OH (R-4)	PHTHN	100.21d	69.75	55.94d	66.65	71.80d	65.59	56.08	—	—	—	—	—	131.70d	123.35d	134.19	168.50d	—

[a] Phthalimido.
[b] d. Doublet.
[c] *N*-2′,4′-Dinitrophenylamino.
[d] Methyl 2-*O*-acetyl-4,6-*O*-benzylidene-3-deoxy-α-D-altropyranosid-3-yl-amino.

Table 3. ^{1}H–^{1}H and ^{1}H–^{13}C coupling constants (Hz) of amino sugar derivatives

Derivative	R-2	R-3	$J_{1,2}$	$J_{1,3}$	$J_{1,5}$	$J_{2,3}$	$J_{2,4}$	$J_{3,4}$	$J_{3,5}$	$J_{3,6}$	$J_{4,5}$	$J_{5,6}$	$J_{5,6'}$	$J_{6,6'}$	$^{1}J_{C\text{-}1,H\text{-}1}$	Others
1	NH_2	OH	1.1	1.1	0.6	2.9	0.4	3.0	0.6	0.7	9.8	5.1	10.4	10.2	168.5	$^{4}J_{PhCH,Ph\ H\text{-}2,6}$ 0.5
2	PHTHN[a]	OH	1.7	0.6	0.6	2.3	<0.5	3.8	—	0.7	9.8	5.1	10.3	10.2	172.6	$^{3}J_{3,HO\text{-}3}$ 2.4
3	OH	DNPNH[b]	1.4	0.7	0.5	3.1	<0.5	3.7	—	0.5	9.9	5.1	10.3	10.4	169.9	$^{3}J_{2,HO\text{-}2}$ 5.9 $^{3}J_{3,NH}$ 8.7
4	OMe	DNPNH	1.2	0.7	0.5	3.1	<0.5	3.6	—	0.5	9.8	5.1	10.3	10.3	170.2[c]	$^{3}J_{3,NH}$ 8.5
5	OAc	DNPNH	1.2	0.7	0.7	2.9	<0.5	3.5	—	0.6	9.8	5.0	9.8	10.4	172.6	$^{3}J_{3,NH}$ 8.5
6	OAc	Alt*p*NH[d]	1.1	1.1	0.6	2.9	<0.5	3.8	—	0.7	9.6	5.2	10.2	9.8	171.0[e]	$^{3}J_{3(3'),NH}$ 8.4
7	OH	NH_2	3.7	<0.5	0.6	9.8	<0.5	9.9	—	<0.5	9.1	4.6	10.4	9.9	169.3	$^{4}J_{PhCH,Ph\ H\text{-}2,6}$ 0.7
8-^{15}**N**	OH	PHTHN	6.9	<0.5	<0.5	8.8	0.3	9.3	0.4	<0.5	10.1	5.0	9.8	10.5	167.2	$^{3}J_{2,HO\text{-}2}$ 3.6
9	OH(R-4)	PHTHN	2.8	0.3	<0.5	1.9	1.1	2.6	0.8	<0.5	2.5	0.9	3.0	9.7	173.1	$^{3}J_{4,HO\text{-}4}$ 11.5

[a] Phthalimido.
[b] *N*-2′,4′-Dinitrophenylamino.
[c] From Ref. 56.
[d] Methyl 2-*O*-acetyl-4,6-*O*-benzylidene-3-deoxy-α-D-altropyranosid-3-yl-amino.
[e] Measured by ^{1}H-coupled 2D HSQC.

molecular dynamics result displayed in Fig. 3a). The highly selective and anti-phase nature of HSQMBC NMR spectra are illustrated in Figure 2, in which only the H-1, H-2, H-3, and H-4 multiplets (resulting from ^{15}N interactions) are detected in a 1D $^{1}H/^{15}N$ HSQMBC spectrum of **9**. Compounds **7** and **9** exhibit uncommon examples of a heteronuclear, W-type long-range coupling (0.6–1.1 Hz) between H-1 and N-3 (Table 4). In most cases, the values of $^{3}J_{HCCN}$ determined by HSQMBC agree with those measured from 1D ^{1}H NMR spectra of ^{15}N-labeled compounds within ±0.2 Hz. However, the values of $J_{2,N\text{-}3}$ measured for **8**-^{15}**N** are a notable exception (Table 4). Because of this discrepancy, we regard the extraction of $^{3}J_{HCCN}$ from 1D ^{1}H spectra of ^{15}N-labeled derivatives as a more reliable method than HSQMBC. Nevertheless, the latter method was essential for measurement of couplings of ^{15}N at natural abundance. It is possible that the presence of proton-exchange processes close to the coupled nuclei of interest affects their relaxation phenomena, thus modifying the *J* values measured by HSQMBC.

Molecular dynamics models of **1**–**8** suggest that the favored orientation of the phenyl ring is orthogonal to the plane of the 4,6-*O*-benzylidene ring, and that the methoxyl group is in the *exo* relationship to the pyranose ring (e.g., see Fig. 3b and c). Also, the MD model of the $^{4}C_1$ pyranoid form of **2** (Fig. 3b) suggests that there is some splaying of the large, axial phthalimido group away from the axial H-4 and axial p-orbital on O-5, with the result that the $\varphi_{1,N\text{-}2}$ and $\varphi_{3,N\text{-}2}$ values in **2** are ∼10° smaller that those in the 2-amino-2-deoxy derivative **1** (see Table 4). This type of conformational distortion of **2** would cause enlargement of the $^{1}H/^{1}H$ dihedral angle $\varphi_{1,2}$ to ∼80°, thus giving a smaller $J_{1,2}$. However, experimentally, $J_{1,2}$ 1.7 Hz is larger for **2** than that (1.1 Hz) for **1**. The reason for this inconsistency could be that compound **2** exists in a conformational equilibrium that contains a minor proportion of a $^{1}S_5$ skew boat form in which $\varphi_{1,2}$ is ∼171°, for which by analogy with the 3-phthalimido derivative **8**, a value $J_{1,2} \sim 7$ Hz would be expected. Significantly, methyl 4,6-*O*-benzylidene-2-deoxy-2-*C*-pentachlorophenyl-α-D-altropyranoside (**10**) has been shown to adopt predominantly a boat form for its pyranoside ring,[27] and we have calculated that the molecular volume of **10** is 341 Å^3, which is larger than the value 297 Å^3 computed for the 2-deoxy-2-phthalimido derivative **2**, owing to the larger size of the pentachlorophenyl group, as compared with the phthalimido substituent.[29] An indication of the free-energy difference between the $^{4}C_1$ chair and $^{1}S_5$ skew forms of **2** was obtained by molecular dynamics with simulated annealing from 1000 K to 300 K by 50 K decrements (CVFF forcefield with implicit solvent), which suggested that the $^{4}C_1$ form is 1.7 kcal/mol more stable than the $^{1}S_5$ form. From $\Delta G = -RT\ln K$, this energy difference corresponds to a population of 95% for the $^{4}C_1$ form. Measurement of the molecular dynamics model of the $^{1}S_5$ form of **2** indicated $\varphi_{1,N\text{-}2}$ 70° and $\varphi_{3,N\text{-}2}$ 36°, which at a population of 5% are expected to have a negligible effect on interpretation of $J_{1,N\text{-}2}$ and $J_{3,N\text{-}2}$. However, if $J_{1,2}$ is estimated to be 1.3 Hz for the $^{4}C_1$ form, and 7.0 Hz for the $^{1}S_5$ form, then the weighted average for 95:5 proportions of these forms is 1.6 Hz, which is comparable with the observed value $J_{1,2}$1.7 Hz for **2**. From molecular dynamics, the $^{4}C_1$ and $^{1}S_5$ forms of **2** of lowest energy both appear to have HO-3 hydrogen bonded to O-4.

Dimer **6** has high symmetry, and only single ^{1}H and ^{13}C NMR spectra were obtained at 11.8 T for the two identical residues, as had also been observed[32] at 8.5 T (360 MHz). The methyl 2-*O*-acetyl-4,6-*O*-benzylidene-3-deoxy-α-D-altropyranosid-3-yl-amino group on one pyranose ring does not count as a large substituent, and so both pyranosyl residues in **6** adopt the $^{4}C_1$ form. Molecular dynamics computations for **6** suggested the presence of a conformational equilibrium about the C-3–N-3 bonds, in which $\varphi_{3,NH}$ values were 178° and 79° in one conformer, and 79° and 178° in another. Thus, the single value $^{3}J_{3,NH}$ 8.4 Hz that was observed is likely an averaged value.

Table 4. $^{1}H–^{15}N$ and $^{13}C–^{15}N$ coupling constants (J, Hz) and $^{1}H–^{15}N$ dihedral angles ($\varphi_{x,N-y}$, deg.)[a] of amino sugar derivatives

	R-2	R-3	$J_{1,N-2}$ $\varphi_{1,N-2}$	$J_{2,N-2}$	$J_{3,N-2}$ $\varphi_{3,N-2}$	$J_{4,N-3}$	$J_{5,N-3}$ $\varphi_{5,N-3}$	$J_{4,N-3}$ $\varphi_{4,N-3}$	$J_{C-1,N-2}$	$J_{C-2,N-2}$	$J_{C-3,N-2}$	$J_{C-1'6'N-2}$[b]	$J_{C-2'5'N-2}$	$J_{C=O,N-2}$	$J_{C-1,N-3}$	$J_{C-2,N-3}$	$J_{C-3,N-3}$	$J_{C-4,N-3}$	$J_{C-5,N-3}$	$J_{C-1'6'N-3}$	$J_{C-2'5'N-3}$	$J_{C=O,N-3}$	Others	$\varphi_{3,NH}$
1	NH_2	OH	1.2 46	0.9	1.4 47	—	—	—	—	—	—	—	—	—	—	—	—	—	—	—	—	—	—	
2-^{15}N	PHTHN	OH	1.2 (1.5)[c] 36	2.1 (2.1)	1.7 (nd[d]) 38	—	—	—	—	1.5	9.7	1.4	8.0	0.8	12.2	—	—	—	—	—	—	—	—	
6	OAc	AlpNH[e]	—	—	—	—	1.3 50	3.4	2.9 172	—	—	—	—	—	—	—	—	—	—	—	—	—	$^{1}J_{HN-3}$ 81.5 $^{3}J_{3,NH}$ 8.4	178, 79[f]
7	OH	NH_2	—	—	—	1.1 171,175[g]	2.8 57	nd	2.3 57	—	—	—	—	—	—	—	—	—	—	—	—	—	—	
8-^{15}N	OH	PHTHN	—	—	—	—	3.9 (2.0) 39	1.4 (1.3)	2.1 (2.3) 142	—	—	—	—	—	—	1.8	nd	10.0	0.6	—	6.1	1.1	12.7	—
9-^{15}N	OH	(R-4) PHTHN	—	—	—	0.8 (0.6) 172,174[g]	1.1 (1.0) 52	1.3 (1.3)	2.6 (2.5) 10	—	—	—	—	—	—	1.5	nd	9.3	nd	0.9	7.8	0.8	12.4	—

[a] Dihedral angles were computed by molecular dynamics/molecular mechanics with an estimated error of ±1°.
[b] Atoms labeled with primes refer to the aromatic ring of the phthalimido group (PHTHN).
[c] Values of $^{1}H–^{15}N$ coupling constants in parentheses (±0.1 Hz) were measured from 1D ^{1}H NMR spectra of ^{15}N-labeled derivatives, and unparenthesized values (±0.2 Hz) by 1D $^{1}H/^{15}N$ HSQMBC of unlabeled compounds.
[d] Not detected.
[e] Methyl 2-*O*-acetyl-4,6-*O*-benzylidene-3-deoxy-α-D-altropyranosid-3-yl-amino.
[f] $\varphi_{3,NH}$ in the two residues alternated between these two values in the molecular dynamics calculations.
[g] Dihedral angles $\varphi_{1,C-3}$ and $\varphi_{C-1,N-3}$, respectively.

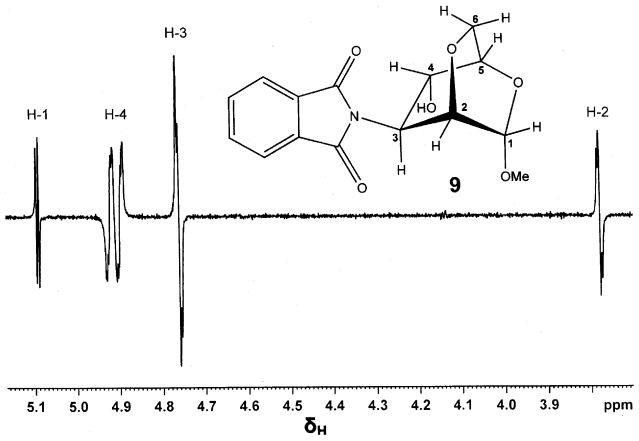

Figure 2. Natural abundance 1D $^{1}H/^{15}N$ HSQMBC NMR spectrum of methyl 2,6-anhydro-3-deoxy-3-phthalimido-α-D-mannopyranoside (**9**), (30 mg) in $CDCl_3$ (0.5 mL) at 500.1/50.7 MHz.

A 2D HSQMBC method was necessary for measurement of the J_{HCCN} values for the *N*-2′,4′-dinitrophenyl derivatives **3**–**5**, because the amino sugar N-3 is coupled to protons in both the sugar and 2′,4′-dinitrophenyl rings. Dispersion of the ^{15}N chemical shifts in the F_1 dimension allowed separation of the cross multiplets of H-3′, H-5′, and H-6′ with the nitro N-2′ and N-4′ nuclei from the cross multiplets of these protons with N-3 (Fig. 4). Measurement of the J_{HCCN} values was performed from multiplets in the 1D slices (e.g., Fig. 5) of the 2D HSQMBC spectra. The 1D and 2D HSQMBC spectra of **3**–**5** yielded a wealth of ^{15}N NMR data that are reported in Table 5, together with single and dual values of dihedral angles computed by molecular dynamics. In the MD models of **3**–**5** (e.g., that of **5** in Fig. 3c) the phenyl and 2′,4′-dinitrophenyl rings are in a stacked orientation, perhaps more as a consequence of the physical space requirements of these large groups, rather than π–π interaction. However, the $^{1}H–^{1}H$ coupling constants of **3**–**5** (Table 3) indicate a strong preference for the $^{4}C_1$ form of the pyranose ring, and, therefore, that the 2′,4′-dinitrophenylamino group is not so large as to cause conformational modification of this form. Hydrogen bonding of the NH with O-1 is also suggested by the MD models of **3**–**5**. Dihedral angles $\varphi_{3',N-2'}$ and $\varphi_{6',N-3}$ of 14–15° for **3**–**5** (Table 5) indicate that the 2′-nitro group is twisted out of the plane of the *N*-2′,4′-dinitrophenylamino group. In Table 5 and Figure 4 may be noted the characteristic ^{15}N chemical shifts of the three types of ^{15}N nuclei in **3**–**5**. The values $^{1}J_{HN-3}$ 92.5–94.8 Hz for **3**–**5** are similar to those of acetamidodeoxy sugars,[36,38,40,41] and are typical of nitrogen atoms that are at least partially sp^2 hybridized. Also noteworthy in Table 5 are the large values 3.8–4.4 Hz observed for the trans coupling $^{3}J_{4,N-3}$ in **3**–**5**, which from MD corresponds to $\varphi_{4,N-3}$ 171–172°.

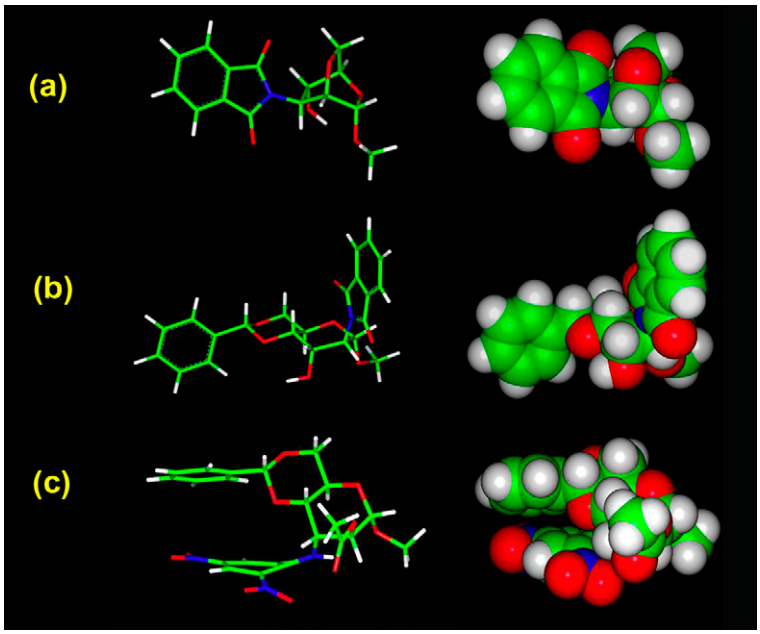

Figure 3. Stick and CPK space-filling models resulting from molecular dynamics/molecular mechanics simulations. (a) Methyl 2,6-anhydro-3-deoxy-3-phthalimido-α-D-mannopyranoside (**9**), (b) methyl 4,6-*O*-benzylidene-2-deoxy-2-phthalimido-α-D-altropyranoside (**2**), and (c) methyl 2-*O*-acetyl-*N*-2′,4′-dinitrophenyl-3-amino-4,6-*O*-benzylidene-3-deoxy-α-D-altropyranoside (**5**).

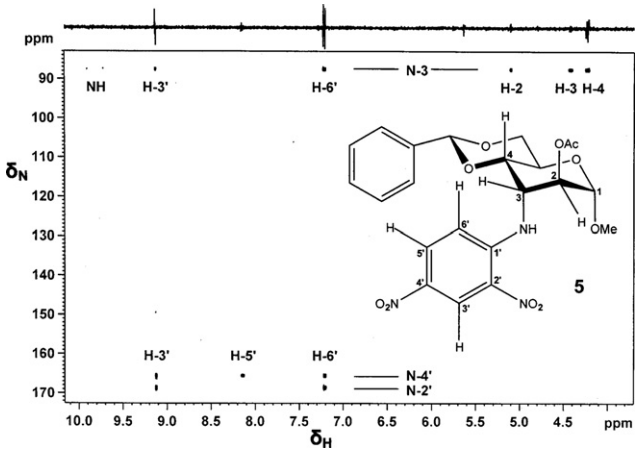

Figure 4. Natural abundance 2D $^{1}H/^{15}N$ HSQMBC NMR spectrum of methyl 2-*O*-acetyl-*N*-2′,4′-dinitrophenyl-3-amino-4,6-*O*-benzylidene-3-deoxy-α-D-altropyranoside (**5**) (30 mg) in $CDCl_3$ (0.5 mL) at 500.1/50.7 MHz; 160 scans/FID over 18.3 h.

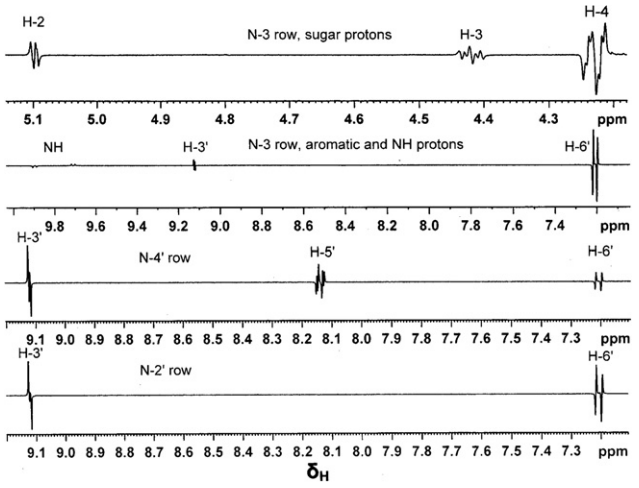

Figure 5. 1D slices (F_2) of the 2D HSQMBC spectrum of **5** shown in Figure 4.

3.2. A Karplus equation for $^{3}J_{HCCN}$

The values of $^{3}J_{HCCN}$ and φ_{HCCN} that were used for a non-linear, least squares fit to the Karplus equation: $^{3}J = A\cos^{2}\varphi + B\cos\varphi + C$ are listed in Table 6, together with an indication of which compounds provided the values. These were judged to be the best values that could be extracted from Tables 4 and 5. Two outliers were eliminated, and the values from derivative **7** were not included because they appear to be examples of a dependence of $^{3}J_{HCCN}$ on electronegativity orientation,[7] a dependence that is not addressed by Karplus equations of the simple, three-parameter type. In the case of ^{1}H–^{1}H couplings[42] and ^{1}H–^{19}F couplings,[43] their dependence on the orientation of electronegative substituents has been treated essentially by creating two equations by use of a 'sign factor', that is given values of either +1 or −1, depending on whether one of the coupled nuclei has a gauche orientation to an electronegative substituent on the attached vicinal carbon atoms, or a trans arrangement with it. This type of dependence can have the effect of doubling the $^{3}J_{HCCH}$ value of

Table 5. ^{15}N NMR parameters and interatomic dihedral angles φ of methyl *N*-2′,4′-dinitrophenyl-3-amino-4,6-*O*-benzylidene-3-deoxy-α-D-altropyranosides **3**–**5**

Parameter	**3**, R = H		**4**, R = Me		**5**, R = Ac	
	J, Hz	φ,[a] deg	*J*, Hz	φ, deg	*J*, Hz	φ, deg
$^{3}J_{2,N\text{-}3}$[b]	1.4	48	0.5	48	1.8	48
$^{2}J_{3,N\text{-}3}$[b]	2.5	—	2.3	—	3.7	—
$^{3}J_{4,N\text{-}3}$[b]	4.4	171	4.2	172	3.8	172
$^{1}J_{HN\text{-}3}$[b]	94.8	—	92.5	—	94.5	—
$^{4}J_{3',N\text{-}3}$[c]	1.1	169, 150	1.2	169, 150	1.2	170, 150
$^{3}J_{6',N\text{-}3}$[c]	2.6	15	2.6	15	2.7	15
$^{3}J_{3',N\text{-}2'}$[c]	2.5	14	2.5	14	2.6	14
$^{3}J_{3',N\text{-}4'}$[c]	2.6	5	2.2	5	2.4	5
$^{3}J_{5',N\text{-}4'}$[c]	0.9	4	1.3	4	0.6	4
$^{4}J_{6',N\text{-}2'}$[c]	2.4	171, 152	2.1	171, 152	2.5	171, 152
$^{4}J_{6',N\text{-}4'}$[c]	2.1	173, 173	2.0	173, 173	2.0	173, 173
	δ_N, ppm[d]		δ_N, ppm		δ_N, ppm	
$\delta_{N\text{-}3}$[c]	89.5	—	89.5	—	87.5	—
$\delta_{N\text{-}2'}$[c]	168.8	—	168.9	—	168.6	—
$\delta_{N\text{-}4'}$[c]	165.9	—	165.9	—	165.6	—

[a] Interatomic dihedral angles φ were determined by molecular dynamics/molecular mechanics computations with an estimated error of ±1°.
[b] Measured by 1D ^{1}H/^{15}N HSQMBC.
[c] Measured by 2D ^{1}H/^{15}N HSQMBC.
[d] ^{15}N chemical shifts δ_N are reported in ppm relative to an external reference of aqueous $^{15}NH_4{}^{15}NO_3$ set to 20.68 ppm, and were measured with a digital resolution of 0.2 ppm/point.

Table 6. Vicinal ^{1}H–^{15}N coupling constants $^{3}J_{HCCN}$ and dihedral angles φ_{HCCN} used for construction of a Karplus equation

Derivative	R-2	R-3	$^{3}J_{HCCN}$ (Hz)	φ_{HCCN}[a] (deg)
9	OH (R-4)	PHTHN[b]	2.6[c]	10
2	PHTHN	OH	1.5	36
			1.7	38
8	OH	PHTHN	1.9	39
1	NH_2	OH	1.2	46
			1.4	47
3	OH	DNPNH[d]	1.4	48
5	OAc	DNPNH	1.8	48
6	OAc	Alt*p*NH[e]	1.3	50
9	OH (R-4)	PHTHN	1.1	52
8	OH	PHTHN	2.3	142
3	OH	DNPNH	4.4	171
5	OAc	DNPNH	3.8	172
4	OMe	DNPNH	4.2	172

The angles are listed in increasing order.
[a] Computed by molecular dynamics/molecular mechanics with an estimated error of ±1°.
[b] Phthalimido.
[c] Coupling constants were measured with an estimated error of ±0.1 Hz by 1D ^{1}H NMR of ^{15}N-labeled compounds, and ±0.2 Hz by 1D and 2D ^{1}H/^{15}N HSQMBC.
[d] *N*-2′,4′-Dinitrophenylamino.
[e] Methyl 2-*O*-acetyl-4,6-*O*-benzylidene-3-deoxy-α-D-altropyranosid-3-yl-amino.

protons having a gauche, electronegative substituent.[7] This effect was also observed for $^{3}J_{HCCN}$ in the present study. For example, the values of $J_{2,N\text{-}3}$ 2.8 Hz and $J_{4,N\text{-}3}$ 2.3 Hz found for **7** are about twice the values $J_{1,N\text{-}2}$ 1.2 Hz and $J_{3,N\text{-}2}$ 1.4 Hz observed for **1** (Table 4), in a case where the group electronegativities are similar. For ^{1}H–^{1}H couplings, some workers have performed Karplus fits containing as many as 11 mutually independent structural terms and 22 adjustable parameters.[11] However, such fits require very large data sets that are beyond the scope of the present study, and in the past, have yielded the conclusion that only four molecular properties are really significant, of which the dihedral angular term is the most important.[11]

Fitting of the data in Table 6 yielded the equation: $^{3}J_{HCCN} = 3.1\cos^2\varphi - 0.6\cos\varphi + 0.4$, which is graphed in Figure 6. In Table 7, the *A*–*C* parameters for this equation are compared with those for 15 other pairs of nuclei, based on equations of the three-parameter type described in the literature. It is seen that the most important variant for different pairs of nuclei is the *A* term,

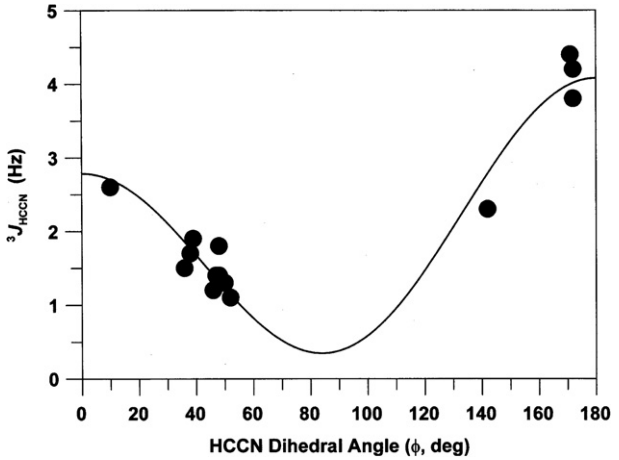

Figure 6. Graph of Karplus equation $^{3}J_{HCCN} = 3.1\cos^2\varphi - 0.6\cos\varphi + 0.4$ obtained by fitting of experimental values of $^{3}J_{HCCN}$ to dihedral angles φ_{HCCN} computed by molecular dynamics simulation.

Table 7. Comparison of Karplus equations of the three-parameter type for different pairs of nuclei separated by three formally saturated bonds, based on the general form of the equation: $^3J = A\cos^2\varphi + B\cos\varphi + C$, and ranked according to the magnitude of A

^3J	A	B	C	Reference
$^3J_{HCNF}$	70.8	−44.1	−7.2	44
$^3J_{CCCSn}$[a]	50.4	−7.6	5.2	57
$^3J_{HCOP}$	15.3	−6.2	1.5	45
$^3J_{HCOH}$	10.4	−1.5	0.2	46
$^3J_{CCOP}$	9.1	−1.9	0.8	47
$^3J_{HCCH}$	9.0	−0.5	−0.3	3
$^3J_{HC\alpha NC'}$	9.0	−4.4	−0.8	48
$^3J_{HCCC}$	8.06	−0.87	0.47	24
$^3J_{HC\alpha NH}$	6.51	−1.76	1.60	49
$^3J_{HCSiH}$	5.83	−2.59	0.84	50
$^3J_{HCOC}$	5.7	−0.6	0.5	19
$^3J_{CCCC}$	4.48	0.18	−0.57	51
$^3J_{HCSC}$	4.44	−1.06	0.45	52
$^3J_{CCOC}$	4.4	1.1	0.5	53
	3.70	0.18	0.11	54
$^3J_{HCCN}$[b]	3.1	−0.6	0.4	This work
$^3J_{HC\alpha C'N}$[b]	−4.6	3.0	0.8	48

[a] ^{119}Sn.
[b] ^{15}N.

which is numerically smallest of all for $^3J_{HCCN}$. However, the magnitudes of $^3J_{HCCN}$ do not scale down from $^3J_{HCCH}$ by as much as a factor of 9.87 (γ_H/γ_N), which means that the measurement of $^3J_{HCCN}$ is not as difficult as might be expected. Although the signs of the $^3J_{HCCN}$ couplings have not been determined in the present work, they are likely to be negative, because of the negative γ_N of the ^{15}N nucleus. In this event, the signs of the parameters A–C might have to be reversed, which would cause the significant A parameter for $^3J_{HCCN}$ couplings to be negative, like that for $^3J_{HC\alpha C'N}$ (see Table 7). However, these couplings are not directly comparable, because $^3J_{HC\alpha C'N}$ includes an sp^2 hybridized carbonyl carbon atom (C′) in the coupling pathway, which could change the magnitude and/or sign of the coupling significantly via a p-orbital contribution. The magnitudes and signs of ^{15}N coupling constants can also be influenced by the presence and orientation of electron lone pairs on nitrogen atoms.[9,55]

4. Summary and conclusions

Vicinal ^{1}H–^{15}N coupling constants have been measured for amino sugar derivatives in known or fixed chair, boat, or skew conformations, either from the 1D ^{1}H NMR spectra of ^{15}N-labeled molecules, or by 1D or 2D ^{1}H/^{15}N HSQMBC NMR spectroscopy of labeled or unlabeled compounds. Complete spectral assignments are reported for all the subject derivatives, the conformations of which are defined by their ^{1}H–^{1}H coupling constants. The geometry of the conformations has been computed by molecular dynamics followed by molecular mechanics energy minimization, and the computed dihedral angles φ_{HCCN} correlated with the values of $^3J_{HCCN}$. Non-linear regression of the $^3J_{HCCN}$ values on the φ_{HCCN} values has yielded a Karplus equation of the simple, three-parameter type: $^3J_{HCCN} = 3.1\cos^2\varphi - 0.6\cos\varphi + 0.4$.

The coefficients in this equation have been compared with literature values for 15 other pairs of coupled nuclei, and the coefficient of the important $\cos^2\varphi$ term found to be the numerically smallest of all for $^3J_{HCCN}$. Based on the history of interpretations of ^{1}H–^{1}H coupling constants,[11,42] Karplus equations of the simple type represent the first stage of a more complex definition of the dependence of such couplings on several molecular parameters, some of which would require a much larger data set, if applied to interpretation of $^3J_{HCCN}$ values.

Acknowledgement

Thanks are due Dr. Wolfgang Bermel for his advice.

References

1. Pozsgay, V.; Coxon, B.; Glaudemans, C. P. J.; Schneerson, R.; Robbins, J. B. *Synlett* **2003**, 743–767.
2. Karplus, M. *J. Chem. Phys.* **1959**, *30*, 11–15.
3. Karplus, M. *J. Am. Chem. Soc.* **1963**, *85*, 2870–2871.
4. Durette, P. L.; Horton, D. *Org. Magn. Reson.* **1971**, *3*, 417–427.
5. Altona, C.; Haasnoot, C. A. G. *Org. Magn. Reson.* **1980**, *13*, 417–429.
6. Haasnoot, C. A. G.; de Leeuw, F. A. A. M.; de Leeuw, H. P. M.; Altona, C. *Org. Magn. Reson.* **1981**, *15*, 43–52.
7. Williams, D. H.; Bhacca, N. S. *J. Am. Chem. Soc.* **1964**, *86*, 2742–2743.
8. Hamman, S.; Beguin, C.; Charlon, C.; Cuong, L.-D. *Org. Magn. Reson.* **1983**, *21*, 361–366.
9. Gil, V. M. S.; von Philipsborn, W. *Magn. Reson. Chem.* **1989**, *27*, 409–430.
10. Altona, C.; Ippel, J. H.; Hoekzema, A. J. A. W.; Erkelens, C.; Groesbeek, M.; Donders, L. A. *Magn. Reson. Chem.* **1989**, *27*, 564–576.
11. Imai, K.; Osawa, E. *Magn. Reson. Chem.* **1990**, *28*, 668–674.
12. Altona, C.; Francke, R.; de Haan, R.; Ippel, J. H.; Daalmans, G. J.; Hoekzema, A. J. A. W.; van Wijk, J. *Magn. Reson. Chem.* **1994**, *32*, 670–678.
13. Lemieux, R. U.; Nagabhushan, T. L.; Paul, B. *Can. J. Chem.* **1972**, *50*, 773–775.
14. Schwarz, J. A.; Perlin, A. S. *Can. J. Chem.* **1972**, *50*, 3667–3676.
15. Hamer, G. K.; Balza, F.; Cyr, N.; Perlin, A. S. *Can. J. Chem.* **1978**, *56*, 3109–3116.
16. Coxon, B. In *Developments in Food Carbohydrate-2*; Lee, C. K., Ed.; Applied Science Publishers Ltd.: Barking, England, 1980; pp 351–390.
17. Cano, F. H.; Foces-Foces, C.; Jiménez-Barbero, J.; Alemany, A.; Bernabé, M.; Martín-Lomas, M. *J. Org. Chem.* **1987**, *52*, 3367–3372.
18. Mulloy, B.; Frenkiel, T. A. *Carbohydr. Res.* **1988**, *184*, 39–46.

19. Tvaroska, I.; Hricovini, M.; Petrakova, E. *Carbohydr. Res.* **1989**, *189*, 359–362.
20. Cloran, F.; Carmichael, I.; Serianni, A. S. *J. Am. Chem. Soc.* **1999**, *121*, 9843–9851.
21. Zhu, Y.; Pan, Q.; Thibaudeau, C.; Zhao, S.; Carmichael, I.; Serianni, A. S. *J. Org. Chem.* **2006**, *71*, 466–479.
22. Perlin, A. S.; Casu, B. *Tetrahedron Lett.* **1969**, 2921–2924.
23. De Marco, A.; Llinas, M. *Biochemistry* **1979**, *18*, 3846–3854.
24. Aydin, R.; Günther, H. *Magn. Reson. Chem.* **1990**, *28*, 448–457.
25. Lichter, R. L.; Roberts, J. D. *J. Org. Chem.* **1970**, *35*, 2806–2807.
26. Coxon, B. *Tetrahedron* **1965**, *32*, 3481–3503.
27. Lee, J. B.; Scanlon *J. Chem. Soc., Chem. Commun.* **1969**, 955–956.
28. Picq, D.; Carret, G.; Anker, D. *Carbohydr. Res.* **1986**, *149*, 458–463.
29. Coxon, B.; Reynolds, R. C. *Carbohydr. Res.* **2001**, *331*, 461–467.
30. Coxon, B. *Carbohydr. Res.* **1999**, *322*, 120–127.
31. Coxon, B.; Reynolds, R. C. *Carbohydr. Res.* **1982**, *110*, 43–54.
32. Coxon, B.; Hough, L. *Carbohydr. Res.* **1979**, *73*, 47–57.
33. Williamson, R. T.; Marquez, B. L.; Gerwick, W. H.; Kover, K. E. *Magn. Reson. Chem.* **2000**, *38*, 265–273.
34. Marquez, B. L.; Gerwick, W. H.; Williamson, R. T. *Magn. Reson. Chem.* **2001**, *39*, 499–530.
35. Homans, S. W. *Biochemistry* **1990**, *29*, 9110–9118.
36. Coxon, B. *Carbohydr. Res.* **1969**, *11*, 153–155.
37. Coxon, B. *Carbohydr. Res.* **1971**, *19*, 197–210.
38. Coxon, B.; Reynolds, R. C. *Carbohydr. Res.* **1980**, *78*, 1–16.
39. Barfield, M. *J. Chem. Phys.* **1964**, *41*, 3825–3832.
40. Coxon, B.; Johnson, L. F. *Carbohydr. Res.* **1971**, *20*, 105–122.
41. Coxon, B. *Pure Appl. Chem.* **1977**, *49*, 1151–1168.
42. Haasnoot, C. A. G.; de Leeuw, F. A. A. M.; Altona, C. *Tetrahedron* **1980**, *36*, 2783–2792.
43. Thibaudeau, C.; Plavec, J.; Chattopadhyaya, J. *J. Org. Chem.* **1998**, *63*, 4967–4984.
44. Hammer, C. F.; Chandrasegaran, S. *J. Am. Chem. Soc.* **1984**, *106*, 1543–1552.
45. Mooren, M. M. W.; Wijmenga, S. S.; van der Marel, G. A.; van Boom, J. H.; Hilbers, C. W. *Nucleic Acids Res.* **1994**, *22*, 2658–2666.
46. Fraser, R. R.; Kaufman, M.; Morand, P.; Govil, G. *Can. J. Chem.* **1969**, *47*, 403–409.
47. Plavec, J.; Chattopadhyaya, J. *Tetrahedron Lett.* **1995**, *36*, 1949–1952.
48. Bystrov, V. F.; Gavrilov, Y. D.; Solkan, V. N. *J. Magn. Reson.* **1975**, *19*, 123–129.
49. Vuister, G. W.; Bax, A. *J. Am. Chem. Soc.* **1993**, *115*, 7772–7777.
50. Carleer, R.; Anteunis, M. J. O. *Org. Magn. Reson.* **1979**, *12*, 673–678.
51. Berger, S. *Org. Magn. Reson.* **1980**, *14*, 65–68.
52. Tvaroska, I.; Mazeau, K.; Blanc-Muesser, M.; Lavaitte, S.; Driguez, H.; Taravel, F. R. *Carbohydr. Res.* **1992**, *229*, 225–231.
53. Milton, M. J.; Harris, R.; Probert, M. A.; Field, R. A.; Homans, S. W. *Glycobiology* **1998**, *8*, 147–153.
54. Bose, B.; Zhao, S.; Stenutz, R.; Cloran, F.; Bondo, P. B.; Bondo, G.; Hertz, B.; Carmichael, I.; Serianni, A. S. *J. Am. Chem. Soc.* **1998**, *120*, 11158–11173.
55. Levy, G. C.; Lichter, R. L. *Nitrogen-15 Nuclear Magnetic Resonance Spectroscopy*; Wiley: New York, 1979; p 117.
56. Coxon, B. *Carbohydr. Res.* **2005**, *340*, 1714–1721.
57. Doddrell, D.; Burfitt, I.; Kitching, W.; Bullpitt, M.; Lee, C.-H.; Mynott, R. J.; Considine, J. L.; Kuivila, H. G.; Sarma, R. H. *J. Am. Chem. Soc.* **1974**, *96*, 1640–1642.